Regular Article

PHYSICAL CHEMISTRY RESEARCH
Published by the
Iranian Chemical Society
www.physchemres.org
info@physchemres.org

***Phys. Chem. Res.**, Vol. 6, No. 2, 309-321, June 2018*
DOI: 10.22036/pcr.2018.104191.1428

Rectification Ratio Enhancement and Functionalized Pyrene: DFT+NEGF

S. Afshari[a,*] and J. Jahanbin Sardroodi[b]

[a]*School of Chemistry, Damghan University, Damghan, Iran*
[b]*Molecular Simulation Lab., Azarbaijan Shahid Madani University, Tabriz, Iran*

(Received 31 October 2017, Accepted 25 February 2018)

Electron transport properties of pure and oxygen and/or methyl substituted pyrene between two semi-infinite aluminum atomic electrodes have been investigated by means of density functional theory plus the non-equilibrium green's function method. The electrodes were represented by a slab of Al atoms oriented along the [111] plane. The computations were carried out in the bias voltage range of 0.0 up to 2.0 V under three gate voltages including -3.0, 0.0 and +3.0 V. The results showed negative differential resistance and relatively high rectification. All of the calculations were carried out with Open source Package for Material eXplorer (OPENMX) 3.6 computer code within the generalized gradient approximation for the exchange-correlation energy and norm-conserving Kleinman-Bylander pseudo potentials. The observed rectifying and the negative differential resistance were justified using the transmission spectrum and its integration in the corresponding bias window. Also, the negative differential resistance behavior was investigated by studying the density of states of left electrode, central region and right electrode and their overlaps.

Keywords: Pyrene, Nano electronic, NDR, Rectifier

INTRODUCTION

With the progress of miniaturization, the components of the electrical circuits used in modern electronic devices swiftly approach molecular scales. The replacement of micrometer-size devices with nanometer-size devices needs transition from the laws of classical mechanics to the laws of quantum mechanics [1]. So, new series of physical phenomena ought to be studied and understood to ease the creation of those devices. Those physical phenomena are the electron transport, single molecule resistance, discrete energy spectrum, zero-bias current, interaction of the external electric fields, *etc*.

Electron transport properties of single-molecule junctions such as conductance, current-bias behavior and transmission spectrum can be obtained by several theoretical calculations. One of the widely-used approaches to the problem is based on density functional theory (DFT) in combination with non-equilibrium Green's function (NEGF) [2] and Landauer's formula [3]. So, many works have shown (experimentally and/or theoretically) that molecular conductance is correlated with molecular length [4,5], conformation[6], functional group effects [7] and other relevent properties .

Besides, many interesting physical properties on current-voltage (I-V) relationship, such as being linear, non-linear, negative differential resistance (NDR), molecular rectifying and electrostatic current switching have been investigated by experimental and theoretical works in the past decade [8-10]. Particularly, the NDR and molecular rectifying properties of many molecular structures are considered as the basic and important properties of the components in the molecular logic electronics and memory circuits [11-15].

Many researchers were interested in studying molecular devices. The first molecular rectifier suggested by Aviram and Ratner (A-R) [16] in 1974. Their conceptual rectifier

*Corresponding author. E-mail: s.fshari@du.ac.ir

was the first molecule acting as an electric circuit element. The A-R rectifier was an asymmetrical organic molecule consisting of two π-electron systems with donor and acceptor properties linked by a σ-bridge. They showed that the difference between the energy levels of the donor and the acceptor parts made possible tunneling in the acceptor to donor direction and significantly hindering in the donor to acceptor direction. Since the suggestion of first molecular rectifier by A-R, many attempts have been made to demonstrate that a suitably designed organic molecule could give current-voltage (I-V) characteristics with the idiographic side-substitution. After that, many molecular rectifiers have been designed using A-R pattern, both theoretically [17-20] and experimentally [21-23].

Graphene is a material to which the highest award in the scientific field has been attributed [24]. It is a single layer of carbon atoms packed in a two-dimensional (2D) honeycomb lattice [25]. It shows peculiar electronic properties arising from its 2D structure and the linear dispersion of the half-occupied π and unoccupied π^* molecular orbitals [26]. These properties such as abnormal quantum Hall effect [27,28] and the ballistic electronic propagation have been handled in a number of applications ranging from nano to macro devices [29-32]. Pyrene is a polycyclic aromatic hydrocarbon consisting of four fused benzene rings, resulting in a flat aromatic system (see Fig. 1a) and with the chemical formula $C_{16}H_{10}$ was supposed to be a hydrogen passivated portion of graphene [33]. In this work the studied molecular nanoelectronics systems are based on pyrene.

There are many studies about electron transport properties of pyrene molecule. The electron transport properties of pyrene by different terminals between Au electrodes [34]. The doping effect on transport properties of the pyrene have been studied by Fan and coworkers [35]. Also, the rectifying and negative differential resistance behaviors based on pyrene have been studied by Zhang and coworkers [36], that the pyrene molecule have been coupled to the asymmetric electrode. They have studied the systems by imposing bias voltage -2.0 to +2.0 V without imposing any gate voltage.

In this regards, study the molecular structures of pure and oxygen and/or methyl functionalized pyrene, using A-R's pattern, seems interesting. So, changing the symmetry of the scattering region by functionalization, and also imposing a gate voltage have been done to study the rectification and transistorized properties, respectively. It could be very useful for designing nanoelectronics devices. The molecular structures shown as structures a and b in Fig. 1 are the structure of pyrene and pyrene between two aluminum atomic electrodes, respectively, also structures c and d are oxygen functionalized and oxygen and methyl functionalized pyrene between two aluminum atomic electrodes, respectively. The IUPAC name of structures b, c and d in Fig. 1 are pyrene, hexa-decahydropyrene-4,10-dione and 5,5,9,9-tetramethyl-hexadecahydropyrene-4,10-dione, respectively. So, for the sake of brevity, hereafter we refer to structures b and c as structures A and B, respectively.

Therefore, in order to investigate the transport properties of the considered structures, the electric current *versus* bias voltage ($I\text{-}V_b$ behavior) has been computed. The studied systems were composed of pyrene, structure A or structure B in contact with two semi-infinite aluminum atomic electrodes from left and right sides. The $I\text{-}V_b$ for the considered systems was computed in the bias range of 0.0-2.0 V. Furthermore, to study the effect of gate voltage on the transport properties different gate voltages including -3.0, 0.0 and +3.0 V was imposed. The results showed exclusive $I\text{-}V_b$ behaviors such as rectifying and NDR characteristic. The validity of the mentioned $I\text{-}V_b$ behaviors has been evaluated using the transmission spectrum and its integral in the bias windows. The NDR behavior has been also investigated by studying the density of states (DOS) of left electrode, central region and right electrode and their overlaps.

METHODS AND MODELS

The system under investigation was a two-terminal nano-electronic electrode-molecule-electrode system in which the right and left electrodes were aluminum atomic electrodes and the molecule at the central region was $C_{16}H_{10}$ (pyrene), $C_{16}H_{10}O_2$ (structure A) or $C_{18}H_{12}O_2$ (structure B). As shown in Fig. 1, three studied molecules were in contact with two Al atomic electrodes extended to electron transfers in z direction. The electrodes were represented by a slab of Al atoms oriented along the [111] plane with 9 atoms per

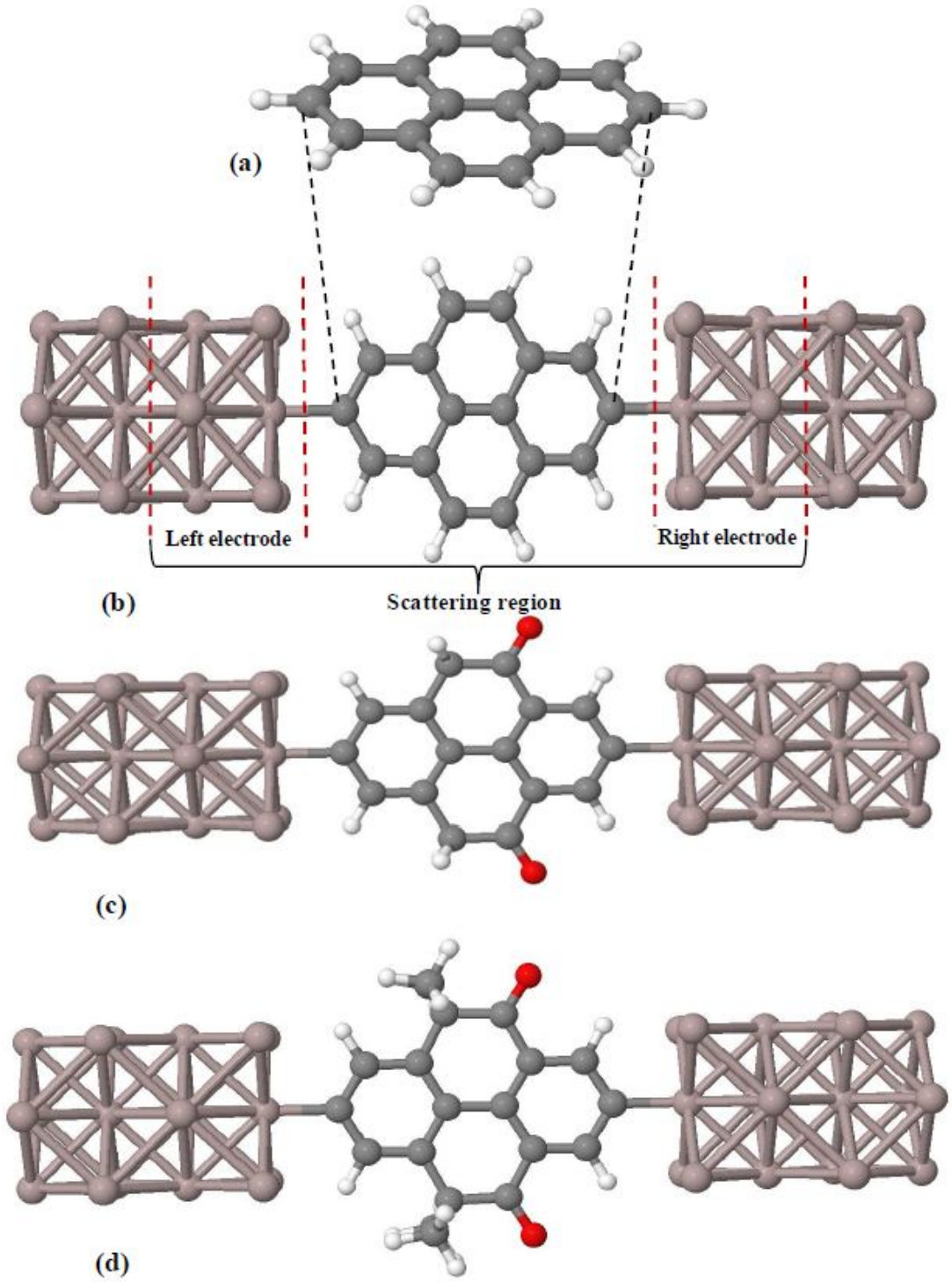

Fig. 1. The schematic geometric structure of a) pyrene, b) pyrene between two aluminum atomic electrodes (pyrene system), c) Oxygen substituted pyrene between two aluminum atomic electrodes (system A) and d) Oxygen and Methyl substituted pyrene between two aluminum atomic electrodes (system B).

unit cell which were repeated to z = ±∞. The carbon atom at the end of the molecule in contact with the electrode was positioned at the top site of electrodes and the distance for a carbon-electrode was 1.90 Å [37]. All computations were carried out at bias voltages ranging from 0.0-2.0 V by imposing the gate voltages (V_g) at the values of -3.0, 0.0 and 3.0 V. The applied gate voltage affects mainly the molecule in the scattering region. The electric potential may resemble the potential produced by the image charges. All of the calculations were carried out with Open source Package for Material eXplorer (OPENMX) 3.6 computer code [38] within the generalized gradient approximation (GGA) [39] for the exchange-correlation energy and Norm-conserving Kleinman-Bylander pseudo potentials [40].

RESULTS AND DISCUSSION

A traditional diode has unique transport characteristics, allowing electrons to be transferred only in one direction. Its resistance is reduced to a small value when the forward bias becomes larger than the threshold voltage, and the resistance is almost infinite under reverse bias. Molecular diodes planned by the A-R model were proposed for the purpose of side-substitution to increase the electron transmission in one direction and decrease in opposite direction. In this work, side-substitution of pyrene was performed with the oxygen and methyl groups in order to intensify the transfer of electron in one direction. So, pyrene and two fictionalized structures derived by substitution of its hydrogens, system A (with two oxygen as electron-acceptor) and system B (with two oxygens, as electron-acceptor, and two methyl groups as electron-donor), with different symmetry in the direction of electron transmission were investigated (see Fig. 1). Before studying these system's transport properties, the central region of systems was optimized by the mentioned method, separately. These three molecules (pyrene, system A and system B) as the central region with two semi-infinite aluminum atomic electrodes were investigated at several bias voltages from -2.0 to +2.0 V. The gate voltages effects on the mentioned molecules were studied by imposing -3.0, 0.0 and +3.0 V, and the gate electrode inducing an external electrostatic potential of the central region. For this purpose the I-V_b curve behavior for the systems have been studied. Because of the symmetry of pyrene molecule, there were not any rectification characteristics for this molecule at the gate voltage 0.0 V. By imposing gate voltages +3.0 and -3.0 V, no rectification characteristics appeared for pyrene system, too. The improved rectification efficiency was more observable from the rectification ratio, as defined in Eq. (1),

$$R = \frac{|I_+|}{|I_-|} \tag{1}$$

where I_+ and I_- are the current at the same amount of positive and negative bias voltages, respectively.

The system "A" has been studied at the gate voltage 0.0 V, too. A close examination of Fig. 2 revealed the nonlinear behavior of the I-V_b curve of this system at that gate voltage. This nonlinear trend contained positive and negative differential resistance (NDR) region in these curves. The considered bias values for the gate voltage 0.0 V, which corresponded to the maxima and minima points in the I-V_b curves, were equal to the values of 10.968 (peak) and 1.048 μA (valley).

For the system A, there was an asymmetry in the electron transport direction in which two hydrogen atoms are substituted by two oxygen atoms (as carbonyl groups) as the electron-acceptor in diagonal direction with respect to the transmission direction (see Fig. 1). It seems that the transmission of electron in one direction is different from that in opposite direction. As can be seen from I-V_b curve in Fig. 3, for this system at gate voltage 0.0 V, the accepting of the electron by the carbonyl groups can not affect enough on the electron transmission and dose not change its properties to diode-like device. So, as can be seen from Fig. 5, changing the rectification ratio of this system is not obvious at gate voltage 0.0 V, but, with imposing the other studied gate voltages (+3.0 and -3.0 V), the I-V_b curves show rectification characteristics. So, the rectification ratio curves (see Fig. 5) have shown specific nonlinear trend characteristics for this system, especially for the gate voltage -3.0 V. In particular, when the bias was increased to 1.8 V, the rectification ratio raised to as high as about 5.85 for the mentioned gate voltage. Then, it decreased to about 1 for bias voltage 2.0 V. On the other hand, this system shows the I-V_b characteristic, NDR, at the gate voltage -3.0 V. These differential resistances or the slope of the I-V_b curves were dependent on the values of the imposed

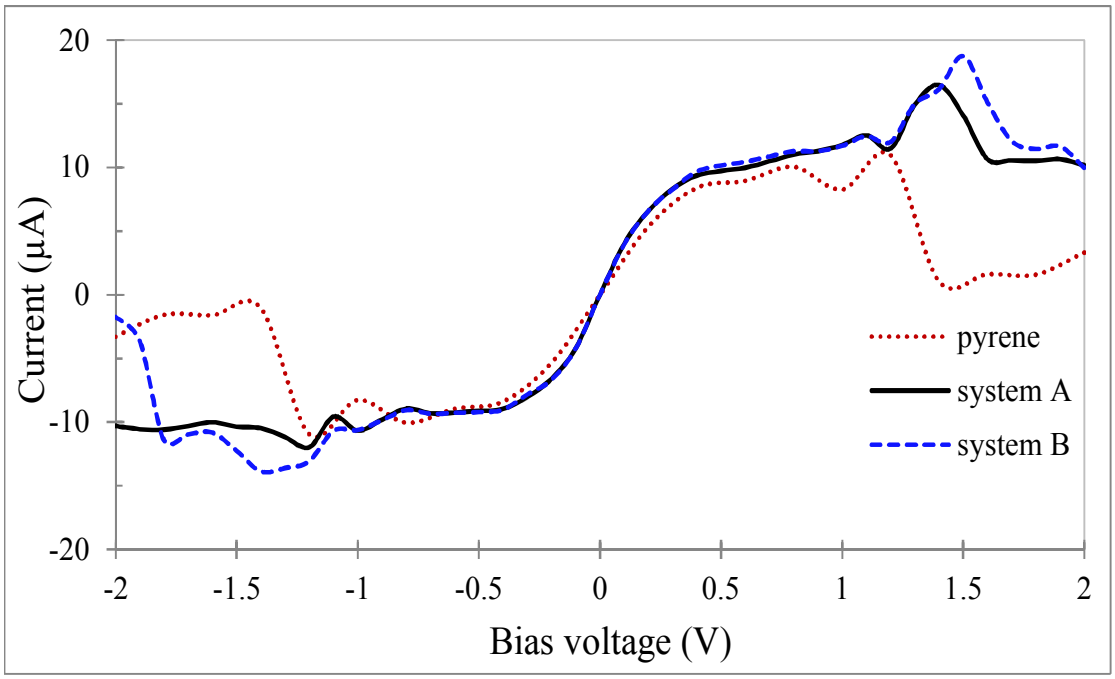

Fig. 2. Current-bias voltage curves for the pyrene, system A and system B with the gate voltage 0.0 V.

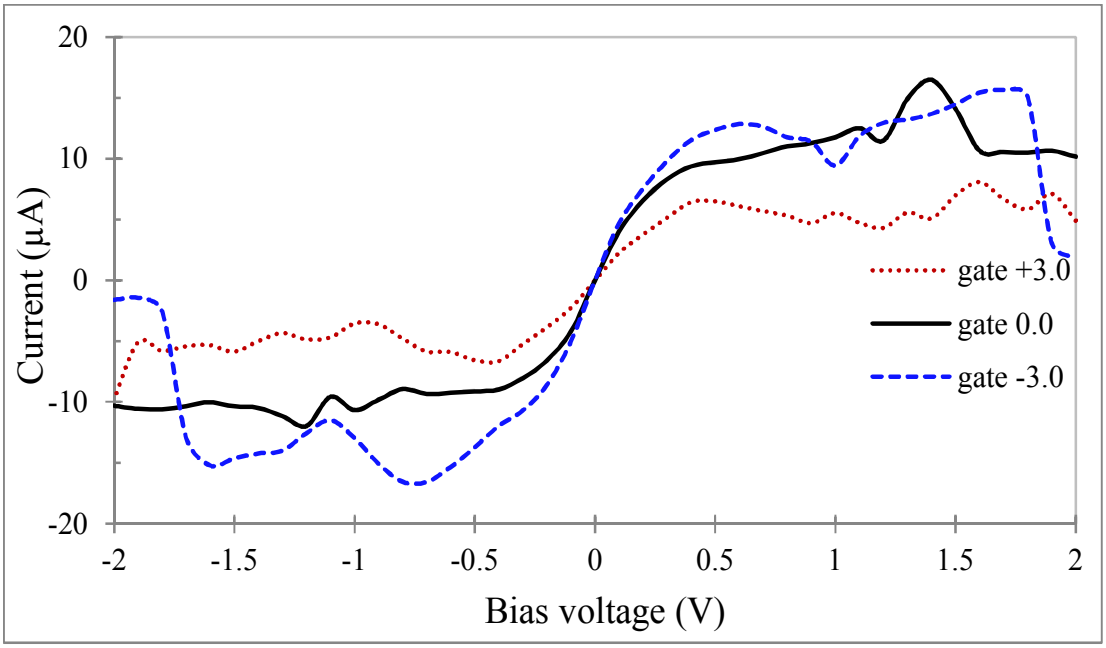

Fig. 3. Current-bias voltage curves with the imposed gate voltages -3.0, 0.0 and +3.0 V for the system A.

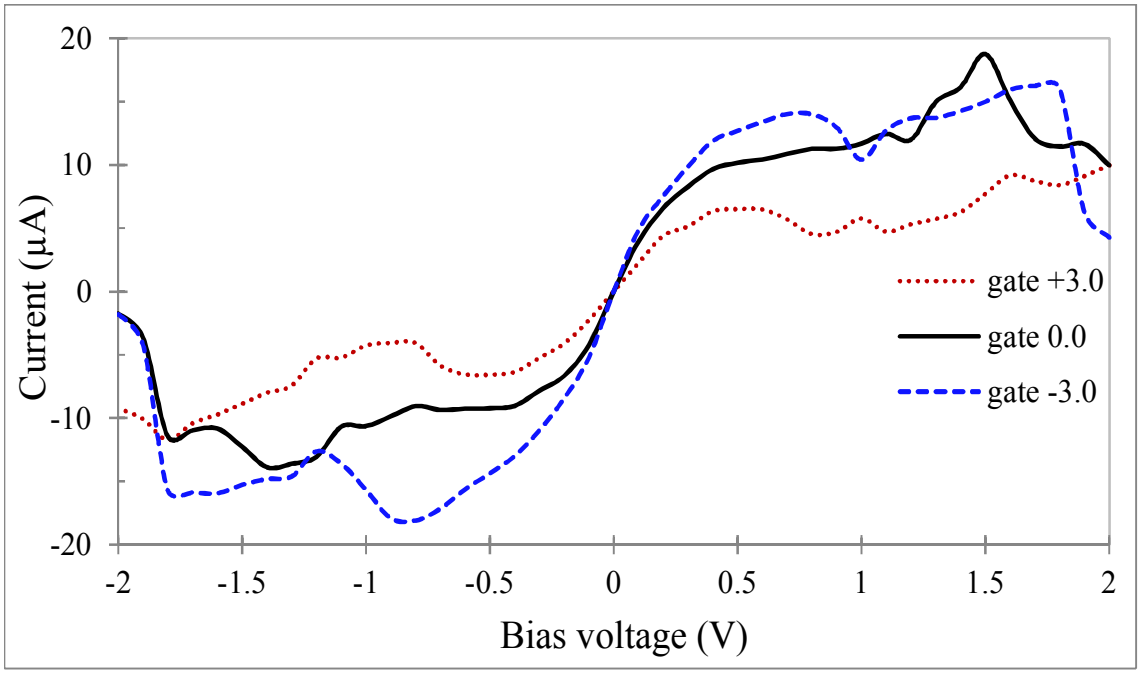

Fig. 4. Currents-bias voltage curves with the imposed gate voltages -3.0, 0.0 and +3.0 V for the system B.

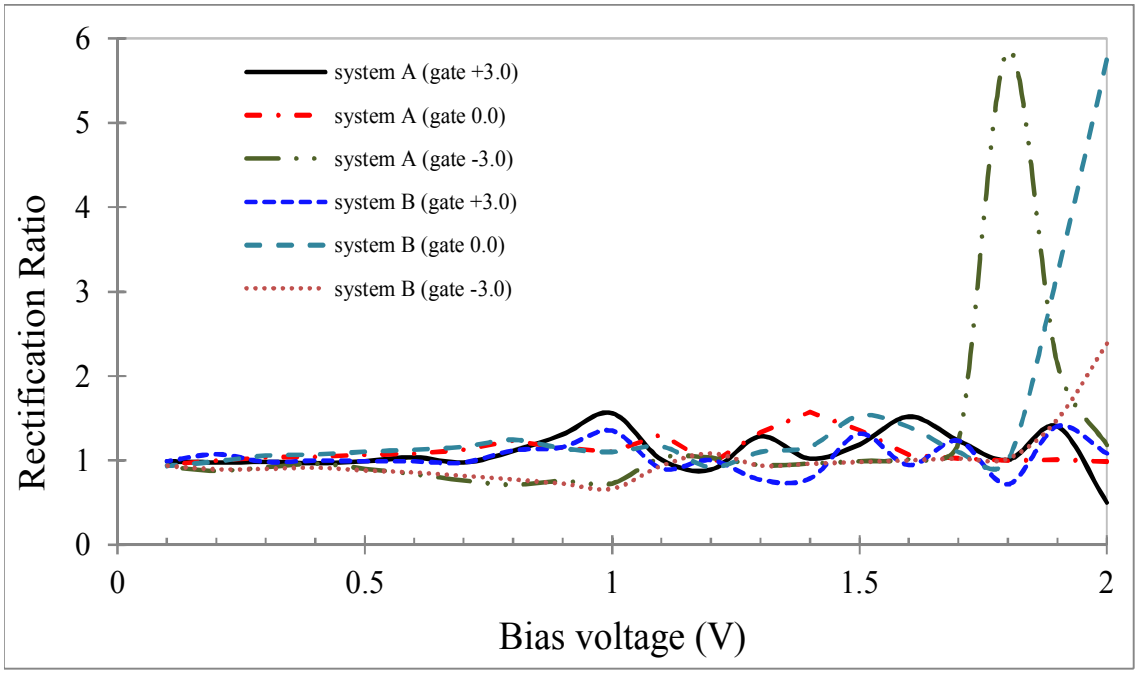

Fig. 5. The bias-dependent rectification ratio for the system A and B with the imposed gate voltages -3.0, 0.0 and +3.0 V.

gate-voltages. This was because there was not any obvious NDR at the other imposed gate voltages (0.0 and +3.0 V). The considered bias values, corresponding to the maxima and minima points in the I-V_b curves, were related to gate voltage -3.0 V and equal to the values of 15.663 (peak) and 1.905 μA (valley) for the positive current area and -16.560 (peak) and -1.425 μA (valley) for the negative current area. Finally, for the system B, there was asymmetry in the electron transporting direction, where two carbonyl groups were on one side as electron-acceptor and four methyl groups as electron-donor were on the opposite side. It seemed that the transmission of electron in one direction differed from that against direction. As can be seen from Fig. 4, the I-V curve showed that there were rectification characteristics. Also, the rectification ratio curves (see Fig. 5) showed specific characteristics of this system. In particular, when the bias was increased to 2.0 V, the ratio was raised to as high as about 2.4 and 5.8 for the gate voltages -3.0 and 0.0 V, respectively. On the other hand, for this system, the obtained I-V_b curves showed NDR with gate -3.0 and 0.0 V, while there was not any obvious NDR with gate voltage +3.0 V. The considered bias values, corresponding to the maxima and minima points in the I-V_b curves, were equal to 16.258 (18.756) as peak and 4.265 (9.977) μA as valley for the positive current area and -18.087 (-13.877) as peak and -1.789 (-1.735) μA as valley for the negative current area with V_g = -3.0 (V_g = 0.0 V).

The transmission function, T(E), was computed for the studied systems at the mentioned bias voltages and gate voltages. This quantity was determined by the scattering rate of the channel region located at the contact between the two electrodes. The conductance was evaluated for the systems at the equilibrium by the help of the transmission function at the Fermi level, E_F, via the following equation:

$$G = G_0 T(E_F) \quad (2)$$

where G and G_0 are the conductance and the fundamental quantum conductance unit (equal to $2e^2/h$), respectively.

By using the transmission formula, the current was determined by the integration of T(E) over electron energy in the bias window.

$$I = \frac{e}{h}\int dE T(E)\Delta f(E) \quad (3)$$

For the system A, because of its NDR at the gate voltage -3 V, the transmission spectrum and the bias windows along with the integration areas at the important bias points beside the current curve for the mentioned gate voltage have been presented in Fig. 6. The considered bias values, corresponding to the maxima and minima points in the I-V_b curves, were equal to the values of 12.851 (peak), 9.437 (valley), 15.663 (peak) and 1.905 μA (valley). These figures, nevertheless, showed that the bias voltage was increased from 0.6 to 1.0 and 1.6 to 2.0 V, area under the transmission curve was decreased; on the other hand, from 0.2 to 0.6 and 1.0 to 1.6 V, this area was increased. For system B at gate voltages 0.0 and -3.0 V, the same analyses were performed, however, for brevity, they have not been presented here. So, by these capabilities of mentioned systems, these devices could be used as multi applicable nano-devices such as nano-switch and rectifier controlling by gate voltages.

Also, as mentioned, the rectification ratio can be defined in Eq. (1). Since the integration area of transmission diagrams for bias voltages corresponds to I_+ and I_- are comparable. So, the integration area of transmission diagram at three important biases (2.0, 1.9 and 1.8 V) for system B is shown in Fig. 7. As can be seen from this figure, the integration area under transmission diagram of +1.8 V is similiar to that of -1.8 V. It is in a good agreement with the rectification ratio in 1.8 V, in which the ratio value is close to 1. Also, the integration area of transmission diagram for -1.9 V is decreased with respect to -1.8 V, but for +1.9 V it is the same as +1.8 V. It caused the increase in the rectification ratio to about 2.4. It means that the integration area for +1.9 V is about 2.4 times more than that for -1.9 V. Comparison of the integration area of transmission diagram for 2.0 V and -2.0 V is the same as +1.9 and -1.9 V. So, the integration area for -2.0 V is very smaller than that for +2.0 V. The integration area for -1.9 V is bigger than that for -2.0 V while the integration area for +1.9 and +2.0 is almost the same. So, a close observation of Fig. 7 shows that the rectification ratio

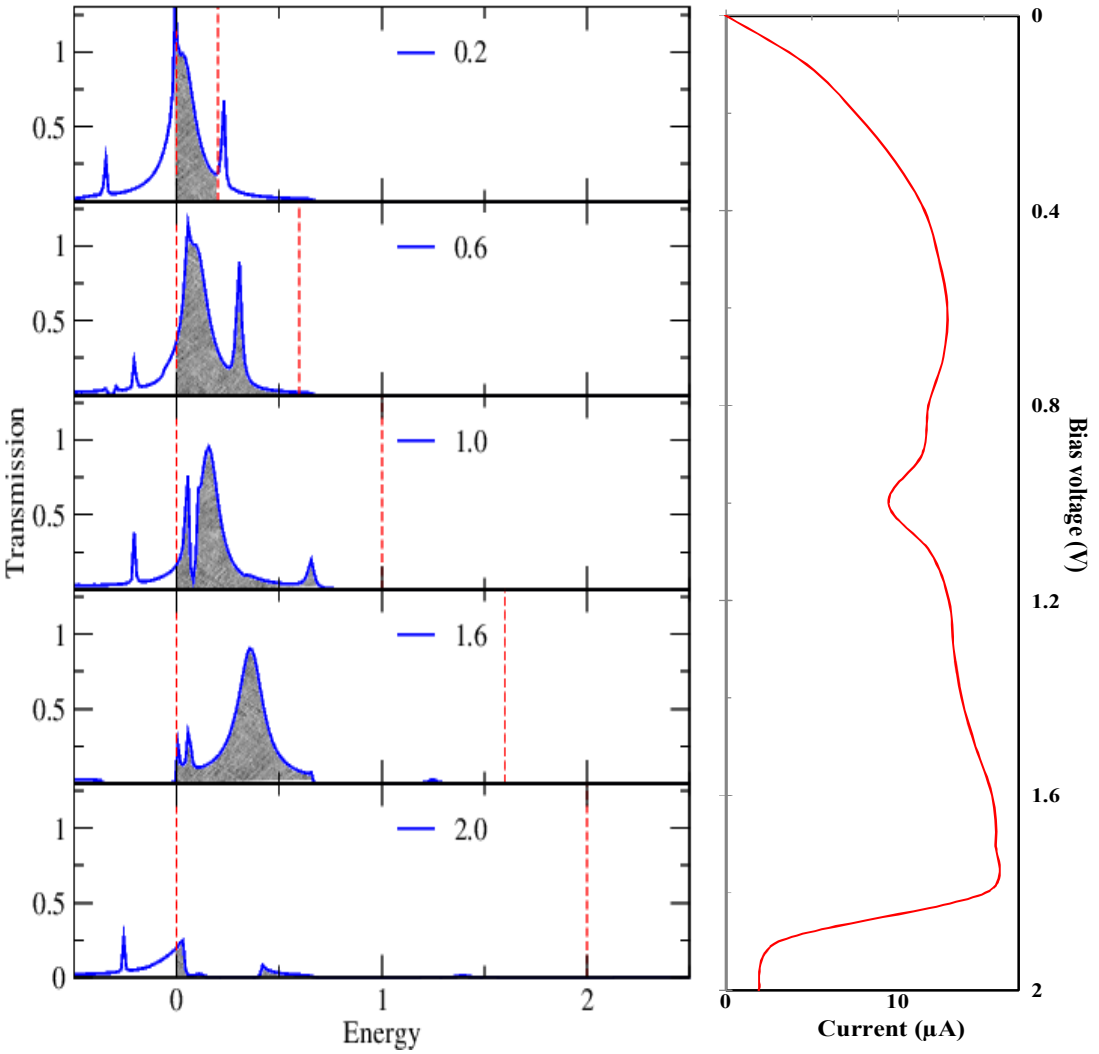

Fig. 6. Integration area of transmission spectrums for system A in the corresponding bias windows in relation with the NDR at the gate voltage -3.0.

for 2.0 V could be more than that for 1.9 V. It shows that the integration area for 2.0 V is about 5.8 times more than that for -2.0 V. This is obvious from the rectification ratio diagram.

To further elucidate the electron transport properties of systems such as NDR behavior the density of states (DOS) for left electrode, central region and right electrode were investigated. This way gives information of how the states contribute to transmission electron during electrode-molecule-electrode system. For simplicity, here just the system A under different bias voltages and the imposing gate voltage -3.0 V is considered and illustrated in Figs. 8a-f. Under zero bias voltage, the DOS of these three parts are the same, as shown in Fig. 8a. The DOS of the electrodes shifts up and down at applied bias voltages for left and right electrodes, respectively. With zero bias voltage, there are many peaks around the Fermi level at central region and also there are states for left and right electrodes, but because of being at the same level of chemical potential energy of the left electrode (μ_L) and right electrode (μ_R), no electron is

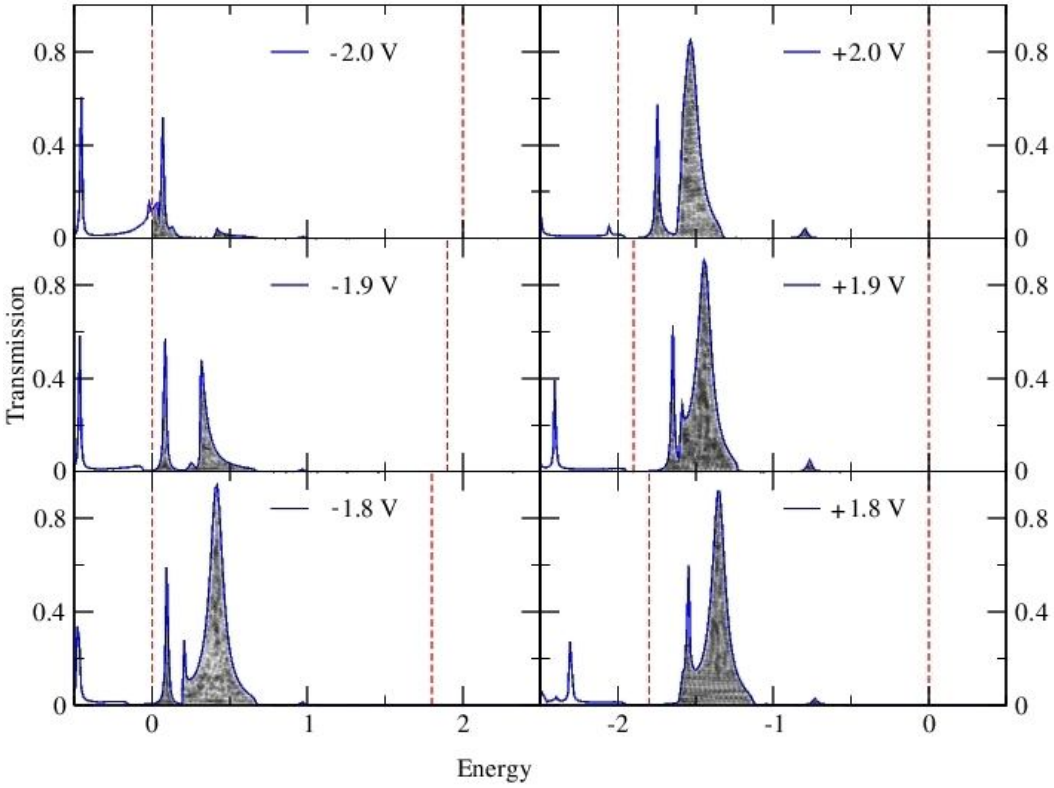

Fig. 7. Integration area of transmission spectrums for the system B in the corresponding bias windows in relation with the rectifying ratio at the gate voltage 0.0 V.

imposed to transport during the system. By imposing a bias voltage the chemical potential of left lead (right lead) increases (decreases) about half amount of bias voltage. By imposing the bias voltage 0.2 V, the chemical potential of the left/right electrodes is increased/decreased about 0.1 eV. Thus, by considering the DOS of the central region, left electrode and right electrode and also the μ_L and μ_R, the transmission of the electron is executable. As can be seen in Fig. 8b, the peaks of DOS around the Fermi level of central region are in the same direction with the valley of the DOS of left and right electrodes. So, the electron could transport slightly. By imposing the bias voltage of 0.6 V, an up-/down-shift of 0.3 V appears in the DOS for left/right electrodes. As can be seen in Fig 8c, the DOS peaks around the Fermi level of central region are in the same direction with the peak of the DOS of right electrode and the valley of the left electrode. Thus, by increasing bias voltage and increasing the overlap between the states of the left electrode and the central region and also, the central region and right electrode, the electron transmission increases that causes the increase in current. The investigation has been continued with bias voltage 1.4 V. So, in this case the states of left lead rise about 0.7 eV and the states of right lead fall to the same amount. The DOS of left electrode, central region and right electrode at bias voltage 1.4 V has been shown in Fig 8d. In this situation, the two sharp peaks of the DOS of the central region around the Fermi level are in the same direction with the broadening peaks of the left and right electrodes. Thus, again by increasing bias voltage and increasing the overlap between the states of the left electrode and the central region and also, the central region and right electrode, the electron transmission increases that causes the increasein current. This trend is also repeated for the bias voltage 1.8 V while it has taken the highest amount

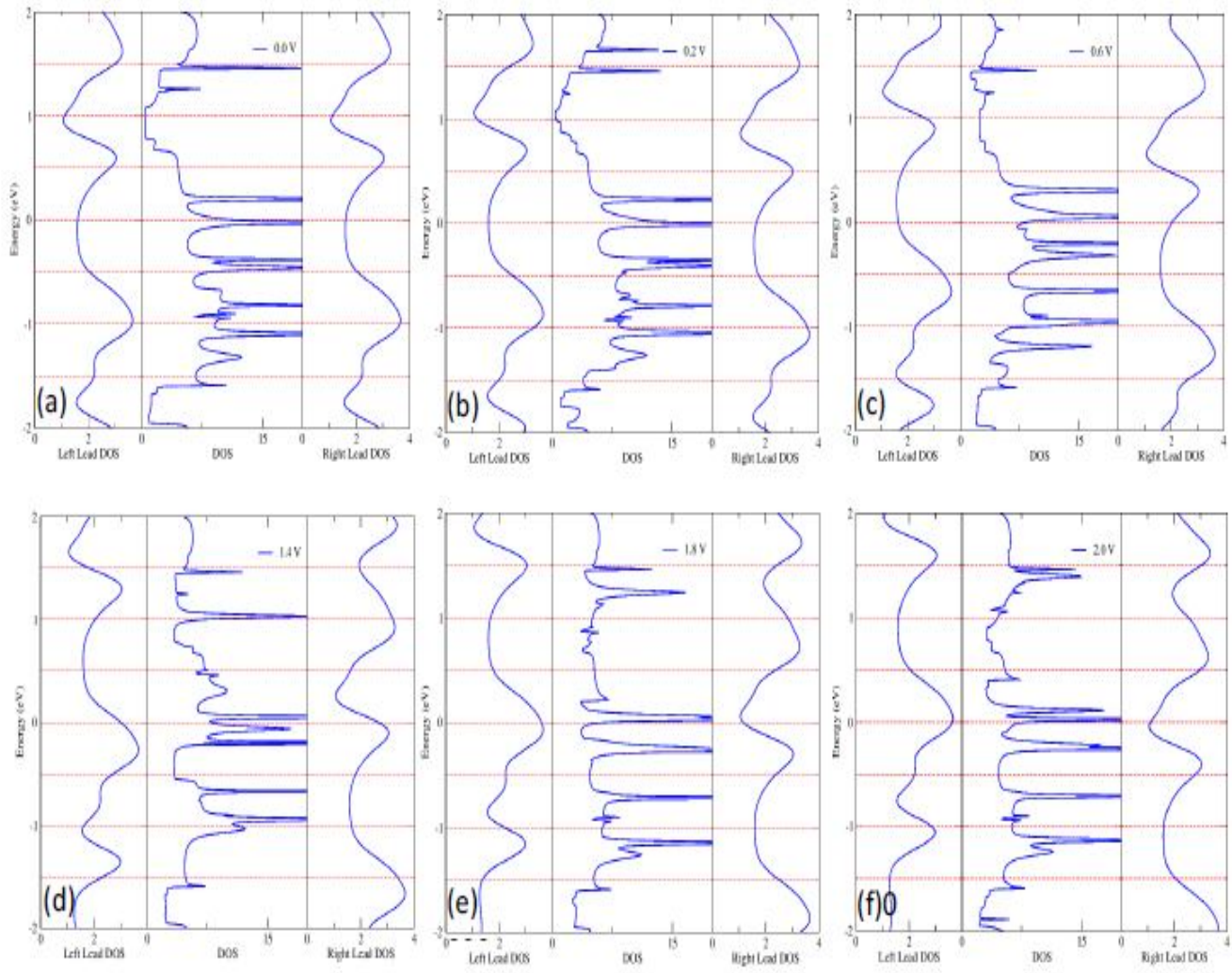

Fig. 8. Density of states for the left electrode, central region and right electrode at a) 0.0, b) 0.2, c) 0.6, d) 1.4, e) 1.8 and f) 2.0 V for the system B at the gate voltage -3.0 V.

of current. In this case, one of the broad peaks of the DOS of central region around the Fermi level is the same direction with the broad peak of the DOS of left electrode and the other one is the same direction with the broad peak of the DOS of right electrode. By more increasing bias voltage and also more increasing the overlap between the states of the left electrode and the central region and also the central region and right electrode the electron transmission is mainly increasedleading, in turn, to a more increasein current (see Figs. 8e and 3). By imposing a bias voltage 2.0 V, it is expected that the current is increased, but, as can be seen from Fig. 3, the current has been decreased. This odd behavior, which is named negative differential resistance, is due to the less overlap between the states of right electrode and the states of the central region. Thus, even with an increase in bias voltage, the electrons could not transport, and so, the current could not increase.

CONCLUSIONS

We have studied the quantum transport properties of pyrene molecule and two fictionalized structures in contact

with two semi-infinite aluminium atomic electrodes. The pyrene's hydrogens have been substituted by oxygen atoms and/or methyl groups. The main purpose of this research was the computational study of the electron donor/acceptor substitution effect on the quantum transport properties. We believe that the electron donor and acceptor substitution cause that the transport in one side differs from that in opposite side. It helps us to have a rectifier as a nano-device. To evaluate the system's electronic properties the effect of the gate voltages at different bias voltages has been studied in this work. The results were presented as the current *versus* the bias voltage curves. Some unique electronic property, such as negative differential resistances and rectifying behavior, are observed. The density of states of the left electrode, central region and right electrode and their overlaps have been investigated to clarify the electron transport of the studied system. Also, on the basis of the results, by imposing the gate voltages, we could have the current-controlling factor in the studied systems. So, these systems could be used as multi applicable nano-devices such as nano-switch and rectifier controlling. To interpret these behaviors, the transmission spectrums, inside the corresponding bias windows, have been compared. Controlling the NDR's occurring bias-range and maximum current value by the structure functionalization and imposing the gate voltage could be regarded as the feasible advantages of a device.

REFERENCES

[1] Carroll, R. L.; Gorman, C. B., The genesis of molecular electronics, *Angew. Chem. Int. Ed. Engl.,* **2002**, *41*, 4378-4400, DOI: 10.1002/1521-3773(20021202)41:23<4378::AID-ANIE4378>3.0.CO;2-A.

[2] Brandbyge, M.; Mozos, J. -L.; Ordejón, P.; Taylor, J.; Stokbro, K., Density-functional method for nonequilibrium electron transport, *Phys. Rev. B.,* **2002**, *65*, 165401-165418, DOI: 10.1103/ PhysRevB.65.165401.

[3] Landauer, R., Spatial variation of currents and fields due to localized scatterers in metallic conduction, *IBM J. Res. Dev.,* **1957**, *1*, 223-231, DOI: 10.1147/ rd.13.0223.

[4] Viljas, J. K.; Pauly, F.; Cuevas, J. C., Modeling elastic and photoassisted transport in organic molecular wires: Length dependence and current-voltage characteristics, *Phys. Rev. B.,* **2008**, *77*, 155119-155133, DOI: 10.1103/PhysRevB.77.155119.

[5] Nozaki, D.; Girard, Y.; Yoshizawa, K., Theoretical study of long-range electron transport in molecular junctions, *J. Phys. Chem. C,* **2008**, *112*, 17408-17415, DOI: 10.1021/jp806806j.

[6] Venkataraman, L.; Klare, J. E.; Nuckolls, C.; Hybertsen, M. S.; Steigerwald, M. L., Dependence of single-molecule junction conductance on molecular conformation, *Nature,* **2006**, *442*, 904-907, DOI: 10.1038/nature05037.

[7] Venkataraman, L.; Park, Y. S.; Whalley, A. C.; Nuckolls, C.; Hybertsen, M. S.; Steigerwald, M. L., Electronics and chemistry: Varying single-molecule junction conductance using chemical substituents, *Nano Lett.*, 2007, *7*, 502-506, DOI: 10.1021/ nl062923j.

[8] Liu, Q.; Luo, G.; Qin, R.; Li, H.; Yan, X.; Xu, C.; Lai, L.; Zhou, J.; Hou, S.; Wang, E.; Gao, Z.; Lu, J., Negative differential resistance in parallel single-walled carbon nanotube contacts, *Phys. Rev. B,* **2011**, *83*, 155442, DOI: 10.1103/ PhysRevB.83.155442.

[9] Fan, Z. -Q.; Chen, K. -Q., Controllable rectifying performance in a C60 molecular device with asymmetric electrodes, *J. Appl. Phys.,* **2011**, *109*, 124505-124517, DOI: 10.1063/1.3597789.

[10] Crljen, Ž.; Grigoriev, A.; Wendin, G.; Stokbro, K., Nonlinear conductance in molecular devices: Molecular length dependence, *Phys. Rev. B,* **2005**, *71*, 165316-165327, DOI: 10.1103/PhysRevB.71.165316.

[11] Dinglasan, J. A. M.; Bailey, M.; Park, J. B.; Dhirani, A. -A., Differential conductance switching of planar tunnel junctions mediated by oxidation/reduction of functionally protected ferrocene, *J. Am. Chem. Soc.,* **2004**, *126*, 6491-6497, DOI: 10.1021/ja0394176.

[12] Yan, Q.; Zhou, G.; Hao, S.; Wu, J.; Duan, W., Mechanism of nanoelectronic switch based on telescoping carbon nanotubes, *Appl. Phys. Lett.,* **2006**, *88*, 173107-173124, DOI:10.1063/1.2198481.

[13] Li, X.; Staykov, A.; Yoshizawa, K., Orbital views of the electron transport through polycyclic aromatic

hydrocarbons with different molecular sizes and edge type structures, *J. Phys. Chem. C,* **2010**, *114*, 9997-10003, DOI: 10.1021/jp102280r.

[14] Kim, W. Y.; Choi, Y. C.; Min, S. K.; Cho, Y.; Kim, K. S., Application of quantum chemistry to nanotechnology: electron and spin transport in molecular devices, *Chem. Soc. Rev.,* **2009**, *38*, 2319-2333, DOI: 10.1039/B820003C.

[15] Xu, Y.; Fang, C.; Ji, G.; Du, W.; Li, D.; Liu, D., Electrostatic current switching and negative differential resistance behavior in a molecular device based on carbon nanotubes, *Phys. Chem. Chem. Phys.,* **2012**, *14*, 668-674, DOI: 10.1039/C1CP22882J.

[16] Aviram, A.; Ratner, M. A., Molecular rectifiers, *Chem. Phys. Lett.,* **1974**, *29*, 277-283, DOI: 10.1016/0009-2614(74)85031-1.

[17] Seminario, J. M.; Zacarias, A. G.; Tour, J. M., Theoretical study of a molecular resonant tunneling diode, *J. Am. Chem. Soc.,* **2000**, *122*, 3015-3020, DOI: 10.1021/ja992936h.

[18] Stokbro, K.; Taylor, J.; Brandbyge, M., Do Aviram−Ratner Diodes Rectify?, *J. Am. Chem. Soc.,* **2003**, *125*, 3674-3675, DOI: 10.1021/ja028229x.

[19] Staykov, A.; Nozaki, D.; Yoshizawa, K., Theoretical study of donor-π-bridge-acceptor unimolecular electric rectifier, *J. Phys. Chem. C,* **2007**, *111*, 11699-11705, DOI: 10.1021/jp072600r.

[20] Liu, H.; Wang, N.; Li, P.; Yin, X.; Yu, C.; Gao, N.; Zhao, J., Theoretical investigation into molecular diodes integrated in series using the non-equilibrium Green's function method, *Phys. Chem. Chem. Phys.,* **2011**, *13*, 1301-1306, DOI: 10.1039/C0CP00118J.

[21] Chen, J.; Reed, M. A.; Rawlett, A. M.; Tour, J. M., Large on-off ratios and negative differential resistance in a molecular electronic device, *Science,* **1999**, *286*, 1550-1552, DOI: 10.1126/science.286.5444.1550.

[22] Chen, W.; Wang, L.; Huang, C.; Lin, T. T.; Gao, X. Y.; Loh, K. P.; Chen, Z .K.; Wee, A. T. S., Effect of functional group (fluorine) of aromatic thiols on electron transfer at the molecule-metal interface, *J. Am. Chem. Soc.,* **2005**, *128*, 935-939, DOI: 10.1021/ja056324a.

[23] Metzger, R. M., Unimolecular rectifiers: Present status, *Chem. Phys.,* **2006**, *326*, 176-187, DOI: 10.1016/j.chemphys.2006.02.026.

[24] Padova, P. D.; Perfetti, P.; Olivieri, B.; Quaresima, C.; Ottaviani, C.; Lay, G. L., 1D graphene-like silicon systems: silicene nano-ribbons, *J. Phys.: Condensed Matter,* **2012**, *24*, 223001-223023, DOI: 10.1088/0953-8984/24/22/223001.

[25] Novoselov, K. S.; Geim, A. K.; Morozov, S. V.; Jiang, D.; Zhang, Y.; Dubonos, S. V.; Grigorieva, I. V.; Firsov, A. A., Electric field effect in atomically thin carbon films, *Science,* **2004**, *306*, 666-669, DOI: 10.1126/science.1102896.

[26] Wallace, P. R., The band theory of graphite, *Phys. Rev.,* **1947**, *71*, 622-634, DOI: 10.1103/PhysRev.71.622.

[27] Zhang, Y.; Tan, Y. -W.; Stormer, H. L.; Kim, P., Experimental observation of the quantum Hall effect and Berry's phase in graphene, *Nature,* **2005**, *438*, 201-204, DOI: 10.1038/nature04235.

[28] Novoselov, K. S.; Geim, A. K.; Morozov, S. V.; Jiang, D.; Katsnelson, M. I.; Grigorieva, I. V.; Dubonos, S. V.; Firsov, A. A., Two-dimensional gas of massless Dirac fermions in graphene, *Nature,* **2005**, *438*, 197-200, DOI: 10.1038/nature04233.

[29] Ossipov, A.; Titov, M.; Beenakker, C. W. J., Reentrance effect in a graphene n-p-n junction coupled to a superconductor, *Phys. Rev. B,* **2007**, *75*, 241401-241412, DOI: 10.1103/PhysRevB.75.241401.

[30] Zhang, L. M.; Fogler, M. M., Nonlinear screening and ballistic transport in a graphene p-n junction, *Phys. Rev. Lett.,* **2008**, *100*, 116804-116810, DOI: 10.1103/PhysRevLett.100.116804.

[31] Lin, Y. -M.; Dimitrakopoulos, C.; Jenkins, K. A.; Farmer, D. B.; Chiu, H. -Y.; Grill, A.; Avouris, P., 100-GHz transistors from wafer-scale epitaxial graphene, *Science,* **2010**, *327*, 662-662, DOI: 10.1126/science.1184289.

[32] Kou, R.; Shao, Y.; Mei, D.; Nie, Z.; Wang, D.; Wang, C.; Viswanathan, V. V.; Park, S.; Aksay, I. A.; Lin, Y.; Wang, Y.; Liu, J., Stabilization of electrocatalytic metal nanoparticles at metal-metal oxide-graphene triple junction points, *J. Am. Chem. Soc.,* **2011**, *133*, 2541-2547, DOI: 10.1021/ja107719u.

[33] Sardroodi, J. J.; Afshari, S.; Ebrahimzadeh, A. R.;

Ghavami, B.; Notash, M. Y., Multi switching behavior of hydrogen passivated silicene as molecular junction: A DFT-NEGF approach, *J. Theoretical and Comput. Chem.,* **2014**, *13*, 1450046-1450057, DOI: 10.1142/s0219633614500461.

[34] Bili, A.; Sanvito, S, Tailoring highly conductive graphene nanoribbons from small polycyclic aromatic hydrocarbons: a computational study, *J. Phys.: Condens. Matter,* **2013**, *25*, 275301-275308, DOI: 10.1088/0953-8984/25/27/275301.

[35] Fan, Z. Q.; Zhang, Z. H.; Qiu, M.; Deng, X. Q.; Tang, G. P., The site effects of B or N doping on I-V characteristics of a single pyrene molecular device, *Appl. Phys. Lett.,* **2012**, *101*, 073104-073109, DOI: 10.1063/1.4745842.

[36] Zhang, H.; Zeng, J.; Chen, K. Q., Rectifying and negative differential resistance behaviors induced by asymmetric electrode coupling in Pyrene-based molecular device, *Physica E,* **2012**, *44*, 1631-1635, DOI: 10.1016/j.physe.2012.04.008.

[37] Larade, B.; Taylor, J.; Mehrez, H.; Guo, H., Conductance, I-V curves, and negative differential resistance of carbon atomic wires, *Phys. Rev. B,* **2001**, *64*, 075420-075430, DOI: 10.1103/ PhysRevB.64.075420.

[38] The code, OPENMX, pseudoatomic basis functions, and pseudopotentials are available on a web site 'http://www.openmxsquare.org'.

[39] Perdew, J. P.; Burke, K.; Ernzerhof, M., Generalized gradient approximation made simple, *Phys. Rev. Lett.,* **1996**, *77*, 3865-3868, DOI: 10.1103/PhysRevLett. 77.3865.

[40] Troullier, N.; Martins, J. L., Efficient pseudopotentials for plane-wave calculations, *Phys. Rev. B,* **1991**, *43*, 1993-2006, DOI: 10.1103/ PhysRevB.43.1993.